Physica B 403 (2008) 3522–3526

Contents lists available at ScienceDirect

Physica B

journal homepage: www.elsevier.com/locate/physb

The effect of impurities on the electronic properties of MgO

Seifollah Jalili [a,b,*], Roya Majidi [c]

[a] Department of Chemistry, K.N. Toosi University of Technology, P.O. Box 16315-1618, Tehran, Iran
[b] Computational Physical Sciences Research Laboratory, Department of Nano-Science, Institute for Studies in Theoretical Physics and Mathematics (IPM), P.O. Box 19395-5531, Tehran, Iran
[c] Department of Physics, Shahid Beheshti University, Tehran, Iran

ARTICLE INFO

Article history:
Received 17 October 2007
Received in revised form
16 May 2008
Accepted 20 May 2008

PACS:
71.15.Ap
71.15.Mb
71.55.−i

Keywords:
Magnesium oxide
Density functional theory
Impurity
Linearized augmented plane wave

ABSTRACT

The effect of impurities on the electronic properties of MgO is investigated using the full potential linearized augmented plane-wave plus local-orbitals method based on density functional theory. The electronic band structures and density of states of MgO in the presence of Ca, Li, and Na impurities were calculated. It is found that increasing the amount of Ca impurity decreases the energy band gap and increases the width of the upper part of the valence band. Some of the considered impurities (Li and Na) change the electronic properties of MgO extensively.

1. Introduction

Alkaline-earth oxides have been widely used in catalysis, electrochemistry, optical fibers, and sensors [1–4]. MgO with its simple rock-salt structure is one of the most significant metal oxides for theoretical and experimental studies. It is known as the most abundant oxide in the earth's lower mantle with a high melting point, as a catalyst in important chemical reactions, and as a good substrate for gas adsorption and high-temperature superconductors [5,6]. In addition, MgO is an ideal candidate for use in optically active devices [3] and composites [5]. Alkaline metals can be easily doped in alkaline-earth oxides and this doping has been found quite useful in industry. For example, when MgO is used as an insulator in nuclear reactors, lithium doping can reduce the radiation damage to the MgO crystal. In addition, Li-doped MgO can be used as a catalyst [7]. In recent years, metal oxides with impurities have been studied extensively. In particular, Stankic et al. reported the solvent-free synthesis of mixed Ca–MgO nanocrystals [8]. Lu et al. [9] have shown the highly reactivity and selectivity of the Li-doped MgO catalyst. The electronic properties of the $Mg_{1-x}Zn_xO$ system were studied by the virtual-crystal approximation for $x<0.5$ in the rock-salt phase [10]. In contrast to the extensive studies, obtaining more information about the electronic properties of doped MgO is useful.

In this paper, we discuss the electronic properties of Ca-, Li-, and Na-doped MgO. This study has been carried out using density functional theory (DFT). For each type of impurity, the electronic band structure and the density of states (DOS) were calculated.

2. Computational method

All calculations were performed using WIEN2K package [11], which is the full potential linearized augmented plane-wave plus local-orbital (FP-LAPW-LO) method based on DFT. The generalized gradient approximation of Perdew–Burke–Ernzerhof 96 was used to include the treatment of the exchange-correlation energy [12]. The separation energy of the valence from the core states is −6 Ry. MgO crystallizes in the sodium chloride structure with lattice constant equal to 4.21 Å. The lattice constant was taken from reported values [13]. We have adopted the same value for the muffin-tin radii of Mg and O ($R_{MT}=1.9$ Bohr) [14]. To achieve energy eigenvalue convergence, we expanded the basis function up to $R_{MT}K_{MAX}=7$ (where K_{MAX} is the maximum modulus for the

* Corresponding author. Tel.: +98 21 22853649; fax: +98 21 22853650.
E-mail address: sjalili@nano.ipm.ac.ir (S. Jalili).

0921-4526/$ - see front matter © 2008 Elsevier B.V. All rights reserved.
doi:10.1016/j.physb.2008.05.030

reciprocal lattice vector). The number of k points in the whole Brillouin zone was chosen as 1000. The iteration process was repeated until the calculated total energy of the crystal converges to less than 10^{-4} Ry.

3. Results and discussion

3.1. Electronic structure of MgO

First, we have studied the electronic properties of MgO and compared our results with available data as a test for our methodology. The calculated electronic band structure along some high-symmetry lines in the Brillouin zone is shown in Fig. 1. The Fermi level (indicated by a horizontal line) lies at zero energy. The minimum of the oxygen s-states is taken about 17.5 eV below the Fermi level at the Γ point. The bottom of the conduction band associated with the magnesium s-states is at 4.8 eV (the Γ point). Both the valence-band maximum and the conduction-band minimum lie at the center of the Brillouin zone; hence we recognize a direct band gap. The calculated band gap energies, E_g, at specific high-symmetry points are given in Table 1 and compared with some available data. Our results and most of the previous calculations predict that $E_g(\Gamma-\Gamma) < E_g(L-L) < E_g(X-X)$. The size of the band gap is 4.8 eV at the Γ point, which is in agreement with other calculations. The calculated band gap is smaller than the experimental value (7.8 eV) [16]. This is a well-known DFT weakness, because DFT only relates to ground-state properties and the band gap itself refers to an excited-state property, which standard DFT is unable to describe correctly [17]. The DOS of MgO is given in Fig. 1. The band width of the upper part of the valence band, E_v, is 4.98 eV. The FP-LAPW method leads to a width of 5 eV [14]. Wang and Holzwarth [18] found a width of 4.8 eV within local-density theory using the self-consistent mixed-basis pseudo-potential techniques. The experimentally determined value of this band width is between 5 and 6 eV [19]. Our results indicate that the adopted method is able to describe the electronic properties of MgO correctly. At normal conditions, MgO has both properties of insulators with a wide band gap and properties of semiconductors with a large valence-band width.

3.2. Structure of doped MgO

To simulate impurities in MgO, we have constructed a super-unit cell by doubling the original simple cubic cell of MgO, corresponding to the stoichiometry of Mg_8O_8. The lattice parameters of this simple tetragonal supercell of MgO are $a = 8.42$ Å and $b = c = 4.21$ Å. First, in this supercell, one of the Mg atoms is replaced by one impurity atom and the electronic properties of doped MgO were investigated. Then the amount of impurity was increased by replacing other Mg atoms by impurities. We placed the impurity atoms at different positions and searched for the most stable positions. For instance, three different structures of $Mg_{0.5}Ca_{0.5}O$ are shown in Fig. 2. The middle configuration is favorable according to its total energy. The stable positions for Li and Na are similar. For $x = 0.5$ (x is the amount of impurity) four impurity atoms are placed at the positions of the Mg atoms 2, 3, 5, and 8.

The possible locations of one single impurity atom in the supercell are equivalent for $x = 0.125$. For $x = 0.25$, two impurity atoms are placed at the positions of the Mg atoms 3 and 5. In addition, the Mg atom 2 (or 8) is replaced by an impurity for $x = 0.375$. The configurations with the impurity atoms close to each other are more stable than other atomic structures. In this paper, we limit our calculations to these special structures.

Table 1
Band-gap energies at some high-symmetry points compared to other calculations (all energies are in eV)

MgO	Γ–Γ	L–L	X–X
Present	4.8	8.6	10.7
FP-LAPW [13]	5.05	8.73	10.32
Pseudo-LDA [14]	4.5	8.0	10.5
APW-LDA [15]	4.98	9.31	9.62

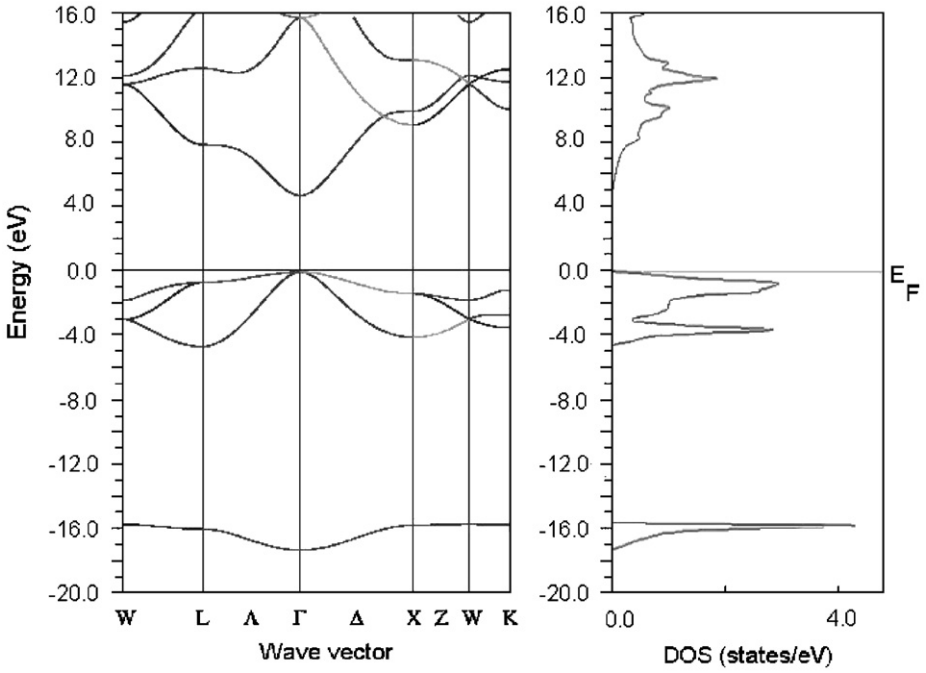

Fig. 1. Electronic band structure and density of states of MgO with face-centered cubic cell.

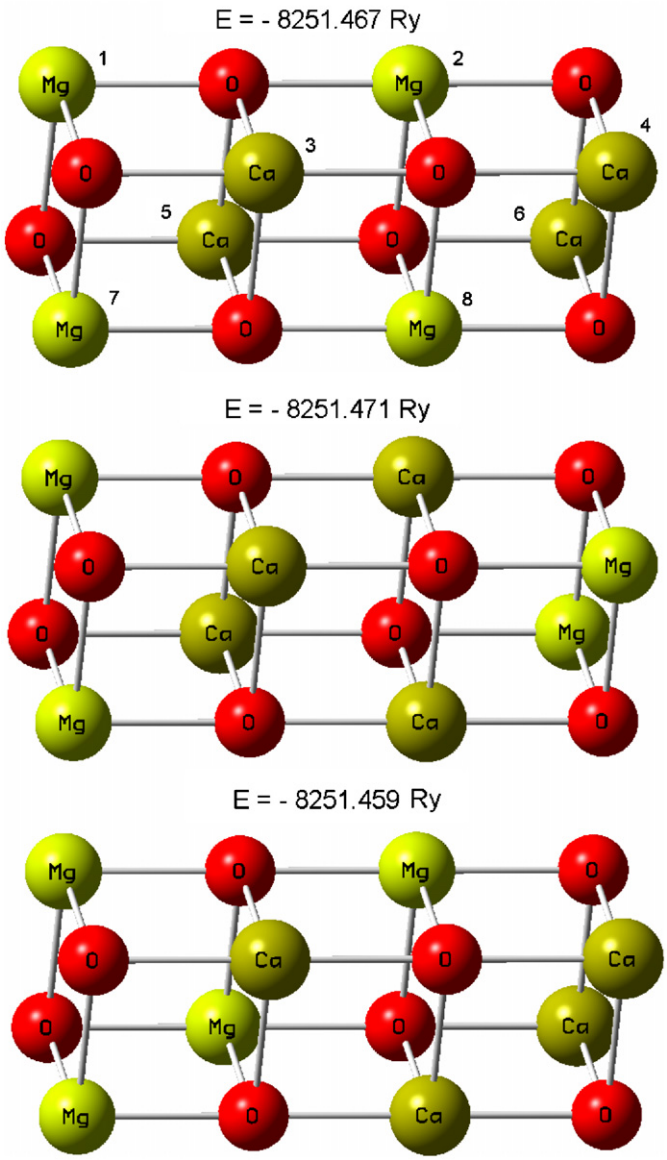

Fig. 2. Three different configurations of $Mg_{0.5}Ca_{0.5}O$.

3.3. *Electronic structures of Ca-, Li- and Na-doped MgO*

First, the electronic properties of the rock-salt CaO are discussed. The top of the valence band and the bottom of the conduction band of CaO are not at the same k point. Accordingly, an indirect band gap of 3.32 eV between the Γ and X points appears in CaO. From the DOS a band width of 2.99 eV is obtained. Our results are in good agreement with earlier calculations, which report a band gap and a band width of 3.46 eV and 3 eV, respectively [14]. Therefore, our method truly predicts the electronic properties of CaO.

To understand the effect of Ca impurity on electronic properties of MgO, the band structures and DOS of $Mg_{1-x}Ca_xO$ for $x \leqslant 0.5$ are shown in Fig. 3. We show only the states that are very close to the Fermi energy, and other levels (near −14 eV) are not presented in the figure. The differences between the electronic properties of MgO and Ca–MgO are very slight. The energy band gap and the band width of the upper valence band of $Mg_{1-x}Ca_xO$ for several impurity contents are given in Table 2. Our results indicate that the energy band gap decreases and the band width of the upper

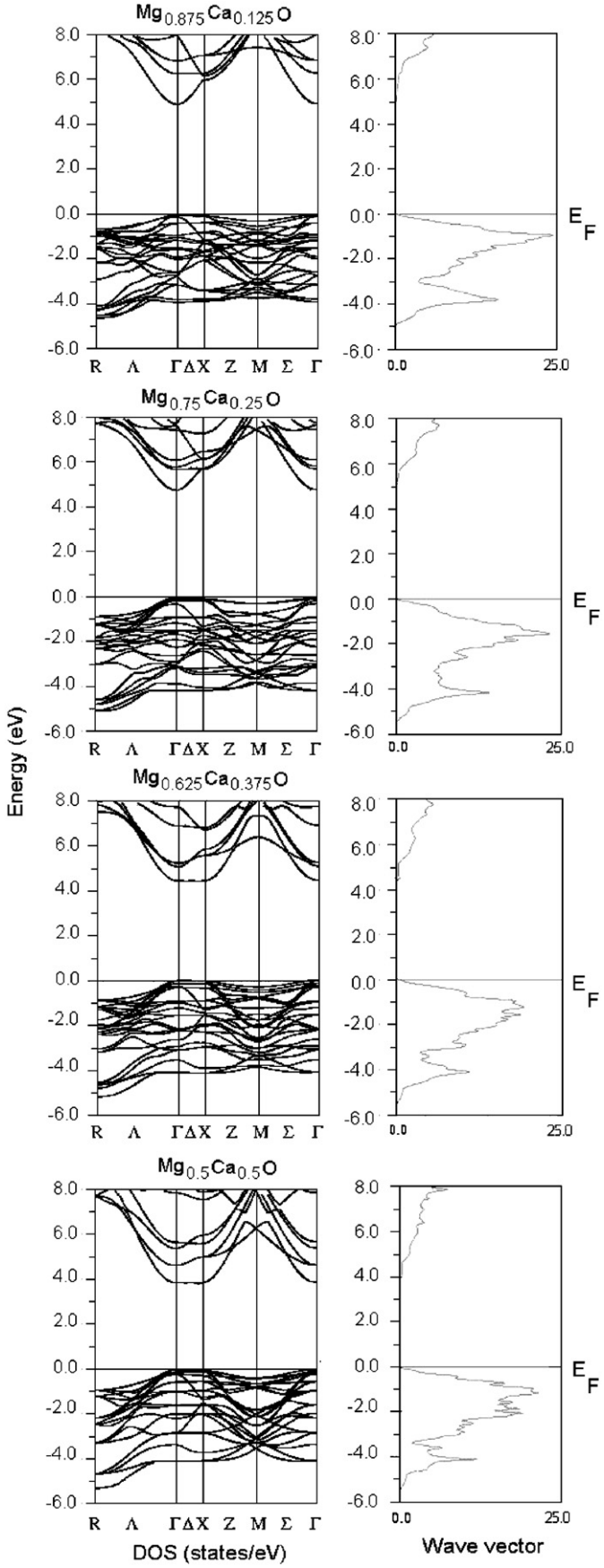

Fig. 3. Electronic band structure and density of states of $Mg_{1-x}Ca_xO$.

Table 2
Band-gap energy and band width of the upper valence band of $Mg_{1-x}Ca_xO$ for $0 \leqslant x \leqslant 1.0$

	E_g	E_v
MgO	4.80	4.98
$Mg_{0.875}Ca_{0.125}O$	4.71	5.14
$Mg_{0.75}Ca_{0.25}O$	4.57	5.63
$Mg_{0.625}Ca_{0.375}O$	4.19	5.74
$Mg_{0.5}Ca_{0.5}O$	3.81	5.80
CaO	3.32	2.99

valence band increases with increasing amount of Ca impurity. There is a small variation in E_g and E_v with x. The atomic number and the number of valence electrons increase in the presence of Ca impurity; thus Ca-doped MgO has larger E_v than pure MgO. The band gap of MgO decreases and gets close to the CaO band gap with increasing amount of Ca impurity. In summary, all $Mg_{1-x}Ca_xO$ are expected to be non-metallic because of a vanishing DOS at the Fermi level; however, Ca impurity has noticeable effects on the conductivity of MgO by changing E_g and E_v.

The electronic properties of MgO in the presence of Li and Na impurity were also studied by using the above procedure. Li- and Na-doped MgO show a difference with Ca-doped MgO. The electronic band structures and DOS of $Mg_{1-x}Na_xO$ for $x \leqslant 0.5$ are shown in Fig. 4. (The results for $Mg_{1-x}Li_xO$ are very similar and not presented here.) Li and Na have one valence electron less than Mg. If one of the Mg atoms is replaced by a Li or Na, one electron is removed. As shown in Fig. 4, the Fermi level crosses many states that were filled with electrons above the Fermi level. Hence, doping with these atoms strongly decreases the number of valence electrons and enhances the electrical conductivity of MgO. In other words, if a Na or Li atom is present in MgO, the unoccupied states above the Fermi level can easily accept electrons from valence band. These impurities are called acceptors. When an electron moves from the valence band to these empty states, a hole is left behind in the valence band. Thus, acceptor levels increase the concentration of the holes by accepting electrons from the valence band. MgO doped with acceptors like Li and Na are known as p-type semiconductors. Comparison between the DOS of Li-doped and Na-doped MgO with pure MgO shows that these impurities affect the value of the DOS at the Fermi level. The widths of the bands above and below the Fermi level (E_{above} and E_{below}) are summarized in Tables 3 and 4. It is found that by increasing the amount of Li and Na impurity, the unoccupied states above the Fermi energy become broad while the width of the occupied states below the Fermi level decreases. The shape of the DOS does not change clearly but the Fermi level moves down through the valence bands as the atomic number and thus the number of valence electrons decreases. The results are in good agreement with the experimental results. Balint et al. have used the defect chemistry equations to describe the formation mechanism of specific lattice defects. It was shown that lithium doping increases the concentration of oxygen vacancies and hence the p-type conduction [20]. Tardío et al. [21] have shown that in Li-doped MgO crystals, the electrical current increases dramatically with an increasing amount of Li impurity.

4. Conclusions

We have investigated the electronic properties of MgO in the presence of impurities (Ca, Li, and Na) using a DFT-based method. Analysis of the band structure and the DOS indicates that MgO is a semiconductor. We have chosen the most stable configurations

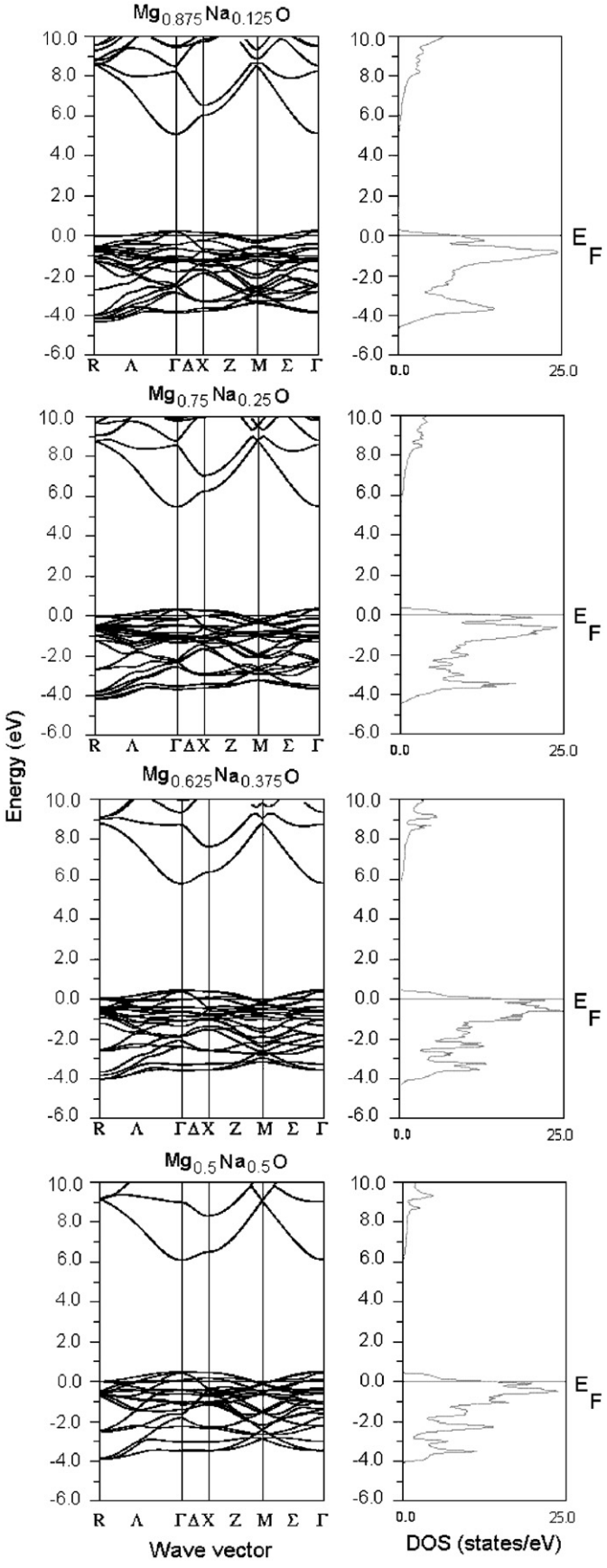

Fig. 4. Electronic band structure and density of states of $Mg_{1-x}Na_xO$.

Table 3
Widths of the bands above and below the Fermi level of $Mg_{1-x}Na_xO$ for $0 \leqslant x \leqslant 1.0$

	E_{below}	E_{above}
$Mg_{0.875}Na_{0.125}O$	4.76	0.39
$Mg_{0.75}Na_{0.25}O$	4.50	0.42
$Mg_{0.625}Na_{0.375}O$	4.37	0.50
$Mg_{0.5}Na_{0.5}O$	4.06	0.56

Table 4
Widths of the bands above and below the Fermi level of $Mg_{1-x}Li_xO$ for $0 \leqslant x \leqslant 1.0$

	E_{below}	E_{above}
$Mg_{0.875}Li_{0.125}O$	4.63	0.26
$Mg_{0.75}Li_{0.25}O$	4.46	0.29
$Mg_{0.625}Li_{0.375}O$	4.43	0.31
$Mg_{0.5}Li_{0.5}O$	3.99	0.41

and investigated their electronic structures. The number of valence electrons and the band width of the upper valence band increase with increasing amount of Ca impurity. The band gap of Ca-doped MgO is smaller than that of pure MgO. Ca impurities increase the conductivity of MgO by changing the E_g and E_v, but we did not find a significant effect on the electronic properties. While Li and Na impurities may cause a large change in the electronic properties of MgO, Li- and Na-doped MgO can exhibit p-type semiconductor behavior.

References

[1] Z. Yang, G. Liu, R. Wu, Phys. Rev. B 65 (2002) 235432.
[2] E.A. Colbourn, Surf. Sci. Rep. 15 (1992) 281.
[3] V.R. Chaudhary, A.M. Rajput, A.S. Mamman, J. Catal. 178 (1998) 576.
[4] S. Stankic, M. Sterrer, P. Hofmann, J. Bernardi, O. Diwald, E. Knözinger, Nano. Lett. 5 (2005) 1889.
[5] G. Bilalbegović, Phys. Rev. B 70 (2004) 45407.
[6] J.Q. Li, Y.J. Xu, Y.F. Zhang, Solid State Commun. 126 (2003) 107.
[7] M.C. Wu, C.M. Truong, D.W. Goodman, Phys. Rev. B 46 (1992) 12688.
[8] S. Stankic, M. Sterrer, P. Hofmann, J. Bernardi, O. Diwald, E. Knözinger, Nano Lett. 5 (2005) 1889.
[9] X. Lu, X. Xu, N. Wang, Q. Zhang, J. Phys. Chem. B 103 (1999) 3373.
[10] D. Fritsch, H. Schmidt, M. Grundmann, Appl. Phys. Lett. 88 (2006) 134104.
[11] P. Blaha, K. Schwarz, G. Madsen, D. Kvasnicka, J. Luitz, WIEN2K, An Augmented Plane Wave Plus Local Orbitals Program for Calculating Crystals Properties, Institute of Physical and Theoretical Chemistry, Vienna, Austria, 2001, ISBN 3-9501031-1-2.
[12] J.P. Perdew, S. Burke, M. Ernzerhof, Phys. Rev. Lett. 77 (1996) 3865.
[13] N.W. Ashcroft, N.D. Mermin, Solid State Physics, Thomson Learning Publication, 1976, p. 80.
[14] H. Baltache, R. Khenata, M. Sahnoun, M. Driz, B. Abbar, B. Bouhafs, Physica B 344 (2004) 334.
[15] K.J. Chang, M.L. Cohen, Phys. Rev. B 30 (1984) 4774.
[16] D.M. Roessler, W.C. Walker, Phys. Rev. 159 (1967) 733.
[17] R. Dronskowski, Computational Chemistry of Solid State Materials, Wiley-VCH GmbH and Co.KgaA, Weinheim, 2005.
[18] Q.S. Wang, N.A.W. Holzwarth, Phys. Rev. B 41 (1990) 3211.
[19] V.S. Stypanyuk, A. Szasz, B.L. Grigorenko, O.V. Farberovich, A.A. Kastnelson, Phys. Status Solidi B 155 (1989) 179.
[20] I. Balint, K.I. Aika, Appl. Surf. Science 173 (2001) 296.
[21] M.M. Tardío, R. Ramírez, R. González, ArXiv: cond-mat/0201502 v1 (2002).